





Cosmology under the fractional calculus approach

Miguel A. García-Aspeitia ¹ ^{*}, Guillermo Fernandez-Anaya ¹ [†], A. Hernández-Almada ² [‡],

Genly Leon ^{3,4} [§], Juan Magaña ⁵ [¶]

¹ Depto. de Física y Matemáticas, Universidad Iberoamericana Ciudad de México, Prolongación Paseo de la Reforma 880, México D. F. 01219, México

² Facultad de Ingeniería, Universidad Autónoma de Querétaro, Centro Universitario Cerro de las Campanas, 76010, Santiago de Querétaro, México

³ Departamento de Matemáticas, Universidad Católica del Norte, Avda. Angamos 0610, Casilla 1280 Antofagasta, Chile

⁴ Institute of System Science, Durban University of Technology, PO Box 1334, Durban, 4000, South Africa

⁵ Escuela de Ingeniería, Universidad Central de Chile, Avenida Francisco de Aguirre 0405, 171-0164 La Serena, Coquimbo, Chile

18 October 2022

ABSTRACT

Fractional cosmology modifies the standard derivative to Caputo’s fractional derivative of order μ , generating changes in General Relativity. Friedmann equations are modified, and the evolution of the species densities depends on μ and the age of the Universe t_U . We estimate stringent constraints on μ using cosmic chronometers, Type Ia supernovae, and joint analysis. We obtain $\mu = 2.839^{+0.117}_{-0.193}$ within the 1σ confidence level providing a non-standard cosmic acceleration at late times; consequently, the Universe would be older than the standard estimations. Additionally, we present a stability analysis for different μ values. This analysis identifies a late-time attractor corresponding to a power-law decelerated solution for $\mu < 2$. Moreover, a non-relativistic critical point exists for $\mu > 1$ and a sink for $\mu > 2$. This solution is a decelerated power-law if $1 < \mu < 2$ and an accelerated power-law solution if $\mu > 2$, consistent with the mean values obtained from the observational analysis. Therefore, for both flat FLRW and Bianchi I metrics, the modified Friedmann equations provide a late cosmic acceleration under this paradigm without introducing a dark energy component. This approach could be a new path to tackling unsolved cosmological problems.

Key words: cosmology: theory, dark energy, cosmological parameters, observations.

1 INTRODUCTION

Modern background cosmology is based on diverse hypotheses, such as the species of fluids. Those species are baryonic matter, photons, neutrinos, and the elusive and mysterious dark matter (DM) and dark energy (DE). In particular, the D.E. component in standard cosmology the well-known Λ CDM model) is considered a cosmological constant (Λ). This mentioned model has several achievements and helps us to describe the late time acceleration observed by Supernovas of the Ia type (SnIa) (Riess et al. 1998) and confirmed by the Cosmic Microwave Background radiation (CMB) (Aghanim & et. al. 2020). On the other hand, Λ CDM describes the structure formation, with an excellent concordance with observations, assuming the presence of cold D.M. Despite these achievements, there are several cracks in their physical and mathematical structure, like the inability to quantify the quantum vacuum fluctuations when we interpret the Λ in this way (Zeldovich 1968; Weinberg 1989). Additionally, the origin of the late time acceleration of the Universe remains unknown (Carroll 2001). On the other hand, the Hubble constant value measured with local observations (see SH0ES Riess et al. (2019)) is

in tension with that estimated from early observations (see Planck Aghanim & et. al. (2020)). A possible alternative to solve this tension is to consider extensions beyond Λ CDM (see Di Valentino et al. (2021a) for a compilation). However, incomprehension between the SnIa absolute magnitude and the Cepheid-based distance ladder instead of an exotic late-time physics could be the reason for the H_0 tension (Efstathiou 2021).

The community searches for extensions to the Λ CDM model to resolve some of the mentioned problems. The approaches to face them are divided into two main branches: i) assume a DE fluid with the capability to accelerate the Universe or ii) modify General Relativity (GR) to obtain the cosmic acceleration without DE (Motta et al. 2021). This paper will focus on the second point under the formalism known as *fractional calculus*, which consists of a generalization of the classical integer order calculus, whose derivatives and integrals are of (real or complex) arbitrary order. These fractional operators are not local. In many cases can model real-world phenomena in a better fashion than those obtained by classical calculation. For example, it is coined fractional dynamics as a field of study in physics and mechanics investigating the behavior of objects and systems that are characterized by power-law nonlocality, power-law long-term memory or fractal properties by us and differentiation of non-integer orders, i.e., by methods in the fractional calculus (see the review Tarasov (2013)). Fractional calculus is a field with multiple applications and a great deal of research activity. Fractional quan-

^{*} E-mail: angel.garcia@ibero.mx

[†] E-mail: guillermo.fernandez@ibero.mx

[‡] E-mail: ahalmada@uaq.mx

[§] E-mail: genly.leon@ucn.cl

[¶] E-mail: juan.magana@ucn.cl

tum mechanics is employed as a tool within quantum field theory and gravity for fractional spacetime (Calcagni 2010a,b) and the fractional quantum field theory at positive temperature (Lim 2006; Lim & Eab 2019) and other applications of quantum cosmology (V. Moniz & Jalalzadeh 2020; Moniz & Jalalzadeh 2020; Rasouli et al. 2021; Jalalzadeh et al. 2021). Recently, the community explores the fractional calculus to tackle problems associated in cosmology (Shchigolev 2011, 2013a,b; Calcagni 2013; Shchigolev 2016; Calcagni 2017a; Shchigolev 2021; Jalalzadeh et al. 2022; Calcagni & De Felice 2020; Calcagni 2021a,b), stochastic GW background (Calcagni & Kuroyanagi 2021), luminosity distance (Calcagni et al. 2019), inflation and CMB spectrum (Calcagni 2017b; Calcagni et al. 2016), Fractional Action Cosmology (El-Nabulsi 2012, 2016a; Jamil et al. 2012), fractional geodesic equation, complex general relativity, and discrete gravity El-Nabulsi (2013b), minimal couplings (El-Nabulsi 2013a), phantom (Rami 2015), Ornstein-Uhlenbeck-like fractional differential equation in cosmology (El-Nabulsi 2016b), a variable Order Parameter (El-Nabulsi 2017a), wormholes in fractional action cosmology (El-Nabulsi 2017c). New metrics were considered (El-Nabulsi 2017b), as well as some dark energy models in emergent, logamediate, and intermediate scenarios of the universe (Debnath et al. 2012, 2013). For instance, Shchigolev (2016, 2021) found $\alpha = 0.926$ (where α is the order of the Riemann-Liouville fractional integral). In Shchigolev (2011, 2013a,b) were obtained several exact solutions for cosmological models, which differs significantly from the standard model due to the fractal nature of spacetime (Calcagni 2010a,b). Jalalzadeh et al. (2022) explore the interval $1 < \alpha < 2$ using Riesz's fractional derivative (that is not related to the index of Riemann-Liouville fractional integral) to obtain the non-boundary and tunneling wave functions for a closed de Sitter geometry. Another example, Barrientos et al. (2021), studies the Universe dynamics without DM and DE components by modifying the mathematical structure of Friedmann equations with fractional calculus. Another approach is calculating the value of the Λ (due to the well-known ultraviolet divergence in the standard quantum field theory), which needs to restructure the theory using the fractional calculus (Calcagni 2021c). In, Giusti (2020); Torres et al. (2020) explore Modified Newtonian Dynamics Theories (MOND) and quantum cosmology in this fractional approach (Barrientos et al. 2021). Finally, notice that there are several definitions of fractional derivatives and fractional integrals, such as those of Riemann-Liouville, Caputo, Riesz, Hadamard, Marchand, and Grünwald-Letnikov, among other more recent ones (see Kilbas et al. (2006), and Podlubny (1998) and references therein). Even though these operators are already well studied, some of the usual features related to function differentiation fails, such as Leibniz's rule, the chain rule, and the semi-group property (Podlubny 1998; Kilbas et al. 2006).

Based on the fractional calculus formalism, a modified Friedmann equation is confronted with data at the background cosmology. In particular, we use Cosmic Chronometers, Type Ia Supernovae observations, and a joint analysis to constrain the fractional parameter. We will show that the term containing the fractional parameter act as a Λ , unveiling that nature can be fractional, and consequently, non-fractional GR is only an approach to the actual mathematical structure of nature. Additionally, we present a dynamical system and stability analysis to explore the phase space for different values of the fractional parameter. Finally, we introduce relevant variables for the model and solve the Friedman restriction locally around the equilibrium points, obtaining a reduced phase plane. Finally, we classify these equilibrium points and provide a range on the fractional parameter to obtain a late-term physical accelerated power-law solution for the scale factor.

The paper is organized as follows: In Sec. 2, we present the mathematical formalism of fractional calculus. In Sec. 3, we show the cosmology based on this theory and how the fractional term could act as a Λ . In Sec. 4, we show the data and methodology we will use to constrain the theory's free parameters. In Sec. 5, we present the results obtained through the different observations and the joint analysis. In Sec. 6, we present a dynamical system and stability analysis of the fractional model. In Sec. 7 we examine the Bianchi I cosmology, presenting a phase space analysis. Finally, in Sec. 8, we give a summary and final discussions. Finally, we will use units where $\hbar = c = k_B = 1$ unless we mention otherwise.

2 MATHEMATICAL FORMALISM FOR FRACTIONAL CALCULUS

Currently, several definitions of fractional derivatives (Uchaikin 2013), like the Riemann-Liouville derivative (R.L.D.), and the Caputo derivative (CD), among others, are used. These derivatives are defined by Cauchy's formula for the integral multiple of integer order $\alpha > 0$, in the form

$${}_c I_t^\alpha f(t) = \Gamma(\mu)^{-1} \int_c^t f(\tau)(t-\tau)^{\alpha-1} d\tau. \quad (1)$$

In this case, the R.L.D. with $\alpha \geq 0$ for $f(t)$ is defined by

$$\begin{aligned} D_t^\alpha f(t) &\equiv \frac{d^n}{dt^n} ({}_c I_t^{n-\alpha} f(t)) \\ &= \Gamma(n-\alpha)^{-1} \frac{d^n}{dt^n} \int_c^t \frac{f(\tau)}{(t-\tau)^{\alpha-n+1}} d\tau, \end{aligned} \quad (2)$$

where $n = [\alpha] + 1$ being $\alpha \in (n-1, n)$. Notice that the main parameter of fractional calculus is given by α , recovering standard calculus when $\alpha \rightarrow 1$. The Caputo left derivative is defined as

$${}_c D_t^\mu f(t) \equiv {}_c I_t^{n-\mu} D_t^n f(t) = \Gamma(n-\mu)^{-1} \int_c^t \frac{\frac{d^n}{d\tau^n} f(\tau)}{(t-\tau)^{\mu-n+1}} d\tau \quad (3)$$

where $n = \begin{cases} [\mu] + 1 & \mu \notin \mathbb{N} \\ \mu & \mu \in \mathbb{N} \end{cases}$. To differentiate the Caputo's fractional constant with the other fractional theories, we denote the fractional constant with the Greek letter μ instead of α .

In fractional calculus, we now have the following relation (see (Uchaikin 2013)) for the case of more than one derivatives

$$D_t^\mu \left[D_t^\beta f(t) \right] = D_t^{\mu+\beta} f(t) - \sum_{j=1}^n D_t^{\beta-j} f(c+) \frac{(t-c)^{-\mu-j}}{\Gamma(1-\mu-j)}, \quad (4)$$

or in other words $D_t^\mu D_t^\beta f(t) \neq D_t^{\mu+\beta} f(t)$, if only not all derivatives $D_t^{\beta-j} f(c+)$ are equal to zero at c . Additionally, the fractional derivative of the Leibniz rule (Uchaikin 2013) reads as

$$D_t^\mu [f(t)g(t)] = \sum_{k=0}^{\infty} \frac{\Gamma(\mu+1)}{k! \Gamma(\mu-k+1)} D_t^{\mu-k} f(t) D_t^k g(t), \quad (5)$$

having the usual when $\mu = n \in \mathbb{N}$.

Finally, we need to mention that in (Shchigolev 2011) and (Roberts 2014), the Riemann curvature tensor and the Einstein tensor are defined as usual, but now with dependence on the μ fractional parameter. In this vein, it is possible to write down the fractional analogous for the Einstein field equation through the expression

$$G_{\alpha\beta}(\mu) = 8\pi G T_{\alpha\beta}(\mu), \quad (6)$$

where $G_{\alpha\beta}(\mu)$ is the Einstein tensor in fractional calculus, and G is the Newton gravitational constant.

In this case, modifications to several astrophysical and cosmological events can be studied. For example, a fractional theory of gravitation for fractional spacetime is developed in (Vacaru 2010, 2012a)). Non-holonomic deformations to cosmology lead to new classes of cosmological models studied in (Vacaru 2012b; Shchigolev 2021).

3 BACKGROUND FRACTIONAL COSMOLOGY

To construct the Lagrangian dynamics, one uses the Fractional Action-Like Variational Approach developed by El-Nabulsi (2005, 2007a,b), El-Nabulsi (2008); and one of the possible versions by Roberts (2014).

3.1 Fractional Action-Like Variational Approach

The background cosmology is based on the Friedmann-Lemaître-Robertson-Walker (FLRW) metric which is written in the form $ds^2 = -N^2(t)dt^2 + a^2(t)(dr^2 + r^2d\Omega^2)$ in where it is considered a flat Universe ($k = 0$) based on Planck observations (Aghanim & et. al. 2020), $a(t)$ is the scale factor and $d\Omega^2 \equiv d\theta^2 + \sin^2\theta d\varphi^2$ is the solid angle. The fractional effective action can be written as

$$S_{\text{eff}} = \frac{1}{\Gamma(\mu)} \int_0^t \left[\frac{3}{8\pi G} \left(\frac{a^2(\tau)\ddot{a}(\tau)}{N^2(\tau)} + \frac{a(\tau)\dot{a}^2(\tau)}{N^2(\tau)} - \frac{a^2(\tau)\dot{a}(\tau)\dot{N}(\tau)}{N^3(\tau)} \right) + a^3(\tau)\mathcal{L}_m \right] (t-\tau)^{\mu-1} N(\tau) d\tau, \quad (7)$$

where $\Gamma(\mu)$ is the Gamma function, \mathcal{L}_m is the matter Lagrangian, μ is the fractional constant parameter, t and τ are the physical and intrinsic time respectively and where the Λ is not considered (see Shchigolev (2011)). Varying the action (7) for $q_i \in \{N, a\}$, we obtain the Euler-Poisson (EP) equations from which are deduced the field equations with a gauge $N = 1$.

The minimization of matter Lagrangian for the energy-momentum tensor for perfect fluid given by $T_{\alpha\beta} = pg_{\alpha\beta} + (\rho + p)u_\alpha u_\beta$, where p , ρ and u_α are pressure, energy density and four-velocity respectively, related through the equation of state (EoS) w as $p = w\rho$, leads to modified Einstein field equations with a perfect fluid source.

Incorporating the several matter sources, the minimization of the fractional action (7) generates the following Raychaudhuri equation (with $N(t) = 1$)

$$\dot{H} + \frac{(\mu-1)H}{2t} + \frac{(\mu-2)(\mu-1)}{2t^2} = -4\pi G \sum_i (p_i + \rho_i), \quad (8)$$

and the Friedmann equation, written in the form

$$H^2 + \frac{(1-\mu)}{t}H = \frac{8\pi G}{3} \sum_i \rho_i, \quad (9)$$

where the sum is over all the species, in this case, matter and radiation. To designate the independent time variables we use the rule $t - \tau = T \mapsto t$ (Shchigolev 2011), where the dots denotes these derivatives. Additionally, the Hubble parameter is defined as $H \equiv \dot{a}/a$. Notice that we are considering that does not exist a Λ and thus, the additional $(1-\mu)Ht^{-1}$ -term of the previous equation should generate the late accelerated expansion.

Moreover, the continuity equation is

$$\sum_i \left[\dot{\rho}_i + 3 \left(H + \frac{1-\mu}{3t} \right) (\rho_i + p_i) \right] = 0. \quad (10)$$

Notice that when $\mu = 1$ in Eq. (9) and (10), the standard cosmology is recovered without Λ .

Using the equation of state $p_i = w_i \rho_i$, where $w_i \neq -1$ are constants, thus we have

$$\begin{aligned} \sum_i (1+w_i) \rho_i \left[\frac{\dot{\rho}_i}{(1+w_i)\rho_i} + 3 \frac{\dot{a}}{a} + \frac{1-\mu}{t} \right] \\ = \sum_i (1+w_i) \rho_i \frac{d}{dt} \left[\ln \left(\rho_i^{1/(1+w_i)} a^3 t^{1-\mu} \right) \right]. \end{aligned} \quad (11)$$

Assuming separated conservation equations for each species considered in the cosmology we have the following equation in differential form,

$$d \left[\ln \left(\rho_i^{1/(1+w_i)} a^3 t^{1-\mu} \right) \right] = 0. \quad (12)$$

Setting $a(t_U) = 1$, where t_U is the age of the Universe, and denoting by ρ_{0i} the current value of energy density of the i -th species, and integrating Eq. (12), we have for each of the species the energy densities

$$\rho_i(t) = \rho_{0i} a(t)^{-3(1+w_i)} (t/t_U)^{(\mu-1)(1+w_i)}. \quad (13)$$

Then, substituting (13) in (9), we obtain

$$H^2 + \frac{(1-\mu)}{t}H = \frac{8\pi G}{3} \sum_i \rho_{0i} a^{-3(1+w_i)} (t/t_U)^{(\mu-1)(1+w_i)}. \quad (14)$$

To compare with the standard model we impose that the universe components are matter ($\rho_1 = \rho_m, w_m = 0$) and radiation ($\rho_2 = \rho_r, w_r = 1/3$), which in our modified scenario evolve as

$$\rho_m = \rho_{0m} a^{-3} (t/t_U)^{\mu-1}, \quad \rho_r = \rho_{0r} a^{-4} (t/t_U)^{\frac{4}{3}(\mu-1)}, \quad (15)$$

respectively, where $\rho_{0m}, \rho_{0r}, a_0 = 1$ are the current values of the energy densities and the scale factor. For $\mu = 1$, the standard calculus is recovered, we have the standard evolution for CDM plus radiation, $\rho_m = \rho_{0m} a^{-3}, \rho_r = \rho_{0r} a^{-4}$ and (14) becomes the standard Friedman equation in term of redshift, $E(z)^2 = \Omega_{0m}(z+1)^3 + \Omega_{0r}(z+1)^4$.

When $\mu \neq 1$, Eq. (14) becomes

$$\begin{aligned} E(z)^2 + (1-\mu) \frac{F(z)}{t_U H_0} E(z) \\ = \Omega_{0m}(z+1)^3 F(z)^{(1-\mu)} + \Omega_{0r}(z+1)^4 F(z)^{\frac{4}{3}(1-\mu)}, \end{aligned} \quad (16)$$

where we have defined $\Omega_{0m} \equiv 8\pi G \rho_{0m}/3H_0^2$, $\Omega_{0r} \equiv 8\pi G \rho_{0r}/3H_0^2$, $E(z) \equiv H(z)/H_0$ and $F(z) \equiv t_U/t(z)$. Note that $F(0) = 1$ due to $t(0) = t_U$, is the age of the universe.

Using the chain rule, we obtain a differential equation for $F(z)$ given by

$$F'(z) = \frac{dt}{dz} \frac{dF}{dt} = \frac{F^2(z)}{t_U H_0 (z+1) E(z)}. \quad (17)$$

When we solve (16) for $E(z)$, two branches are dictated by the sign \pm . The branch $-$ leads to $E \leq 0$ and the branch $+$ leads to $E \geq 0$.

Therefore, since we are interested in an expanding universe, we choose the positive branch. That is,

$$\begin{aligned} E(z) = -fF(z) + F(z)^{-\mu} \left\{ f^2 F(z)^{2(\mu+1)} + \Omega_{0m}(z+1)^3 F(z)^{\mu+1} \right. \\ \left. + \Omega_{0r}(z+1)^4 F(z)^{\frac{2(\mu+2)}{3}} \right\}^{1/2}, \end{aligned} \quad (18)$$

where $f \equiv (1-\mu)/(2t_U H_0)$ is going to be the fractional constant that will act as the cosmological constant. Friedmann constraint gives us $f = (\Omega_{0m} + \Omega_{0r} - 1)/2$, such that for $\mu < 1$, $\Omega_{0m} + \Omega_{0r} > 1$, for $\mu > 1$,

$\Omega_{0m} + \Omega_{0r} < 1$, and notice that we choose the positive branch in order to have $E(z) > 0$ and where $\Omega_{0r} = 2.469 \times 10^{-5} h^{-2} (1 + 0.2271 N_{\text{eff}})$, where $N_{\text{eff}} = 2.99 \pm 0.17$ (Aghanim & et. al. 2020). The condition $\Omega_{0m} + \Omega_{0r} > 1$, can be produced in a closed FLRW universe.

In Eq. (9), the term $(1 - \mu)Ht^{-1}$ contributes as a positive term for $\mu < 1$ or a negative term for $\mu > 1$. Substituting (18) in (17), we obtain a differential equation

$$F'(z) = \frac{2fF(z)^{\mu+2}}{(\mu-1)(z+1)} \times \left\{ fF(z)^{\mu+1} - \left[f^2 F(z)^{2\mu+2} + \Omega_{0m}(z+1)^3 F(z)^{\mu+1} + \Omega_{0r}(z+1)^4 F(z)^{\frac{2(\mu+2)}{3}} \right]^{1/2} \right\}^{-1}, \quad (19)$$

That has to be solved numerically. Then, we numerically calculate (18) plugging back the numerical results for $F(z)$.

Moreover, the deceleration parameter $q(z)$ can be written as

$$q(z) = -1 + (1+z) \frac{d \ln E(z)}{dz}. \quad (20)$$

Hence, substituting (18) in (20), using (17) to replace $F'(z)$, and using (18) to eliminate the radical we obtain a closed form for $q(z)$ as given by Eq. (A1), which quantifies if the Universe is in an accelerated stage and under which conditions.

Finally, the cosmographic parameter known as the *jerk*, which quantifies if the model tends to Λ or its another kind of DE, can be written as

$$j = q(2q+1) + (1+z) \frac{dq}{dz}, \quad (21)$$

where q is given by Eq. (A1).

3.2 Analytic solution to the fractional Friedmann equation

Notice that for $\mu \neq 1$, the modified continuity equation (10), also yields the condition

$$\frac{8\pi G}{3} \sum_i p_i = \frac{2(\mu-3)H}{t} + H^2 - \frac{(\mu-2)(\mu-1)}{t^2}. \quad (22)$$

Combining with (8) and (9), one obtains

$$\dot{H} + \frac{2(\mu-4)H}{t} + 3H^2 - \frac{(\mu-2)(\mu-1)}{t^2} = 0, \quad (23)$$

whose analytical solution is (see an analogous case in Shchigolev (2013a), Eq. (36))

$$H(t) = \frac{9-2\mu}{6t} + \frac{\sqrt{8\mu(2\mu-9)+105} \left(1 - \frac{2c_1}{t\sqrt{8\mu(2\mu-9)+105}+c_1} \right)}{6t}, \quad (24)$$

where

$$c_1 = \frac{t_U \sqrt{8\mu(2\mu-9)+105} \left(-6H_0 t_U - 2\mu + \sqrt{8\mu(2\mu-9)+105} + 9 \right)}{6H_0 t_U + 2\mu + \sqrt{8\mu(2\mu-9)+105} - 9}, \quad (25)$$

is an integration constant depending on μ , the H_0 value and the Universe's age, t_U . The relation between redshift z and cosmic time

t is through the scale factor,

$$a(z) := (1+z)^{-1}$$

$$= \left[\frac{t \sqrt{8\mu(2\mu-9)+105} + c_1}{t_U \sqrt{8\mu(2\mu-9)+105} + c_1} \right]^{\frac{1}{3}} \left[\frac{t}{t_U} \right]^{\frac{1}{6} \left(-2\mu - \sqrt{8\mu(2\mu-9)+105} + 9 \right)}. \quad (26)$$

That also leads asymptotically to power-law scale factors for large t , having

$$a(t) \simeq t^{\frac{1}{6} \left(-2\mu + \sqrt{8\mu(2\mu-9)+105} + 9 \right)}, \quad (27)$$

For $\mu \notin \{1, 2\}$ and for large t , we acquire $q < 0$, and then we have late-time acceleration without DE. The respective $E(t)$ and $q(t)$ parameters are shown in Appendix B.

4 METHODOLOGY AND DATASET

A Bayesian Markov Chain Monte Carlo (MCMC) analysis is performed to constrain the phase-space parameter $\Theta = \{h, \Omega_{0m}, \mu\}$ of the fractional cosmology using observational Hubble data OHD, SNIa dataset and joint analysis. Under the emcee Python package environment (Foreman-Mackey et al. 2013), after the auto-correlation time criterion warranty the convergence of the chains, a set of 4000 chains with 250 steps each is performed to establish the parameter bounds. Additionally, the configuration for the priors are Uniform distributions allowing vary the parameters in the range $h \in [0.2, 1]$, $\Omega_{0m} \in [0, 1]$ and $\mu \in [1, 3]$. Hence the figure-of-merit for the joint analysis is built through the Gaussian log-likelihood given as $-2 \ln(\mathcal{L}_{\text{data}}) \propto \chi^2_{\text{data}}$ and

$$\chi^2_{\text{Joint}} = \chi^2_{\text{CC}} + \chi^2_{\text{SNIa}}, \quad (28)$$

where each term refers to the χ^2 -function for each dataset. Now, each piece of data is described in the rest of the Section.

4.1 Cosmic chronometers

Up to now, a set of 31 points obtained by differential age tools, namely cosmic chronometers (CC), represents the measurements of the Hubble parameter, which is cosmological independent (Moresco et al. 2016). In this sense, this sample is useful to bound alternative models to Λ CDM. Thus, the figure-of-merit function to minimize is given by

$$\chi^2_{\text{CC}} = \sum_{i=1}^{31} \left(\frac{H_{th}(z_i) - H_{obs}(z_i)}{\sigma_{obs}^i} \right)^2, \quad (29)$$

where the sum runs over the whole sample, and $H_{th} - H_{obs}$ is the difference between the theoretical and observational Hubble parameter at the redshift z_i and σ_{obs} is the uncertainty of H_{obs} .

4.2 Type Ia Supernovae

Ref. (Scolnic et al. 2018) provides 1048 luminosity modulus measurements, known as Pantheon sample, from Type Ia Supernovae which cover a region $0.01 < z < 2.3$. Due to this sample, the measurements are correlated, and it is convenient to build the chi-square function as

$$\chi^2_{\text{SNIa}} = a + \log \left(\frac{e}{2\pi} \right) - \frac{b^2}{e}, \quad (30)$$

where

$$\begin{aligned} a &= \Delta\tilde{\mu}^T \cdot \mathbf{Cov}_P^{-1} \cdot \Delta\tilde{\mu}, \\ b &= \Delta\tilde{\mu}^T \cdot \mathbf{Cov}_P^{-1} \cdot \Delta\mathbf{1}, \\ e &= \Delta\mathbf{1}^T \cdot \mathbf{Cov}_P^{-1} \cdot \Delta\mathbf{1}, \end{aligned} \quad (31)$$

and $\Delta\tilde{\mu}$ is the vector of residuals between the theoretical distance modulus and the observed one, $\Delta\mathbf{1} = (1, 1, \dots, 1)^T$, \mathbf{Cov}_P is the covariance matrix formed by adding the systematic and statistic uncertainties, i.e. $\mathbf{Cov}_P = \mathbf{Cov}_{P,\text{sys}} + \mathbf{Cov}_{P,\text{stat}}$. The super-index T on the above expressions denotes the transpose of the vectors.

The theoretical distance modulus is estimated by

$$m_{th} = \mathcal{M} + 5 \log_{10} \left[\frac{d_L(z)}{10 \text{ pc}} \right], \quad (32)$$

where \mathcal{M} is a nuisance parameter which has been marginalized by Eq. (30).

The luminosity distance, denoted as $d_L(z)$, is computed through

$$d_L(z) = (1+z)c \int_0^z \frac{dz'}{H(z')}, \quad (33)$$

being c the speed of light.

5 RESULTS

Table 1 presents the cosmological constraints of fractional cosmology for CC and SNIa, samples and the joint analysis, respectively. Each best-fit parameter value includes uncertainty at 68% confidence level (CL).

Figure 1 shows the 1D marginalized posterior distributions for each data and joint analysis and also the 2D phase space distribution at 68% (1σ), 99.7% (3σ) CL. According to the χ^2 value, the model is in good agreement with the data. Furthermore, the characteristic parameter of the fractional cosmology, μ , is estimated for each dataset, and in particular, we have $\mu = 2.8393^{+0.117}_{-0.193}$ for the joint analysis, allowing an accelerated Universe. Notice that we recover traditional calculus when $\mu = 1$; however, in the region $0 < \mu < 1$, obtaining an accelerated physical Universe (with non-negative “age”) at late stages is not feasible. For this μ -range, we can obtain an accelerated power-law solution corresponding to negative values for the age of the Universe; thus, the corresponding solution is nonphysical. Hence, one way to avoid this affliction is under the introduction of Λ , which will act as a cosmological constant. However, we are in a loop because the idea explains the Universe’s acceleration through the μ term, which contributes to the fractional calculus theory. The other way is to consider $\mu > 2$, and then we get an accelerated physical Universe at late stages.

On the other hand, the age of the Universe is estimated for each dataset, $t_U/\text{Gyrs} = 33.633^{+14.745}_{-15.095}$ (CC), $33.837^{+27.833}_{-10.788}$ (SNIa) and $33.617^{+3.411}_{-4.511}$ (joint). For the Joint value, we obtain around 2.4 times larger than the age of the Universe expected under the standard paradigm, which is also in disagreement with the value obtained with globular clusters, $t_U = 13.5^{+0.16}_{-0.14} \pm 0.23$ (Valcin et al. 2021). The term $(1-\mu)H/t$, which acts as an extra source of mass leading to a closed Universe, could be the origin of this older Universe. In closed scenarios, the Universe becomes older than the standard prediction (Di Valentino et al. 2021b).

Regarding the cosmographic parameters at $z = 0$ we have $q_0 = -0.315^{+0.030}_{-0.028}$ and $j_0 = 0.040^{+0.032}_{-0.053}$ using the joint analysis. Furthermore, the redshift transition between acceleration and deceleration stages of $z_T = 2.388^{+0.610}_{-0.510}$ is estimated. From Figure 2, the

z_T , q_0 and j_0 values for fractional cosmology are deviated more than 3σ to the value obtained by Λ CDM. In contrast to Λ CDM, the reconstruction of a jerk for the alternative cosmology suggests an effective dynamical equation of state for the Universe for late times.

Figure 3 displays the reconstruction of the $H_0(z)$ diagnostic (Krishnan et al. 2021) for the fractional cosmology and its error band at 3σ CL. Although the path (solid line) for the fractional cosmology is consistent within 3σ with the CMB Planck value (Aghanim & et. al. 2020) for $z \lesssim 1.5$, we can observe that it presents a trend to the H_0 value obtained by SH0ES (Riess et al. 2019) for the present time. Nevertheless, the H_0 value for $1.5 < z < 2.5$ is lower than the Planck value, suggesting a tension in this value.

6 DYNAMICAL SYSTEMS AND STABILITY ANALYSIS

Defining the dimensionless age parameter $A = tH$, the re-scaled (dimensionless) energy density $\varrho_i = t^2 \rho_i$ where ρ_i is defined in (13), and the logarithmic time $\tau = \ln t$ such that for any function g we have $dg/d\tau = t dg/dt$.

For the new variables, we have a restriction

$$A^2 + (1-\mu)A = \frac{8\pi G}{3} \sum_i \varrho_i, \quad (34)$$

and evolution equations for each species

$$\frac{d\varrho_i}{d\tau} = \varrho_i (1 + \mu + (\mu - 1)w_i - 3A(w_i + 1)). \quad (35)$$

To compare with the standard model we impose that the universe components are two ($n = 2$), CDM ($\mu_1 = \varrho_m, w_1 = w_m = 0$) and radiation ($\mu_2 = \varrho_r, w_2 = w_r = 1/3$), which in our modified scenario evolve according to

$$\frac{d\varrho_m}{d\tau} = \varrho_m(\mu - 3A + 1), \quad (36)$$

$$\frac{d\varrho_r}{d\tau} = \frac{2\varrho_r(2\mu - 6A + 1)}{3}, \quad (37)$$

$$\frac{dA}{d\tau} = \frac{8\pi G(3(\mu - 3A + 1)\varrho_m + 2(2\mu - 6A + 1)\varrho_r)}{9(1 - \mu + 2A)}. \quad (38)$$

Now, we present a reduced phase space which is determined by a coupled system $d\mathbf{X}/d\tau = \mathbf{F}(\mathbf{X})$ subject to a constraint $G(\mathbf{X}) = 0$ (\mathbf{X} constitute the reduced phase space variables). Of central importance to the investigation of the dynamical system are the equilibrium points which are determined by the equations $\mathbf{F}(\mathbf{X}) = 0, G(\mathbf{X}) = 0$. We calculate the gradient $\nabla G(\mathbf{X})$, that is used to solve the constraint to linear order locally. Defining the dimensionless variables

$$x_1 = \frac{8\pi G\varrho_m}{3\left(A + \frac{|1-\mu|}{2}\right)^2}, \quad x_2 = \frac{8\pi G\varrho_r}{3\left(A + \frac{|1-\mu|}{2}\right)^2}, \quad (39)$$

that evolve as

$$\begin{aligned} \frac{dx_1}{d\tau} &= \frac{x_1}{3-3\mu+6A} \left[-3\mu^2 + 6A^2(3x_1 + 4x_2 - 3) \right. \\ &\quad \left. + |1-\mu|(9Ax_1 + 2x_2(-2\mu+6A-1) - 3(\mu+1)x_1) \right. \\ &\quad \left. - A(-15\mu+6(\mu+1)x_1 + (8\mu+4)x_2 + 3) \right], \end{aligned} \quad (40)$$

$$\begin{aligned} \frac{dx_2}{d\tau} &= \frac{x_2}{3-3\mu+6A} \left\{ 2[-2\mu^2 + \mu + 3A^2(3x_1 + 4x_2 - 4) \right. \\ &\quad \left. - 3(\mu+1)Ax_1 - 2A(-5\mu+2\mu x_2 + x_2 + 2) + 1] \right. \\ &\quad \left. + |1-\mu|(9Ax_1 + 2x_2(-2\mu+6A-1) - 3(\mu+1)x_1) \right\}, \end{aligned} \quad (41)$$

$$\frac{dA}{d\tau} = -\frac{(2A + |1-\mu|)^2(9Ax_1 + 2x_2(-2\mu+6A-1) - 3(\mu+1)x_1)}{12(-\mu+2A+1)}, \quad (42)$$

Sample	χ^2_{\min}	h	Ω_{0m}	μ
CC	16.14	$0.629^{+0.027}_{-0.027}$	$0.399^{+0.093}_{-0.122}$	$2.281^{+0.492}_{-0.433}$
SnIa	54.83	$0.599^{+0.275}_{-0.269}$	$0.160^{+0.050}_{-0.072}$	$2.771^{+0.161}_{-0.214}$
Joint	78.69	$0.692^{+0.019}_{-0.018}$	$0.228^{+0.035}_{-0.040}$	$2.839^{+0.117}_{-0.193}$

Table 1. Best-fit values and their 68% CL uncertainties for fractional cosmology with CC, SnIa and a Joint analysis.

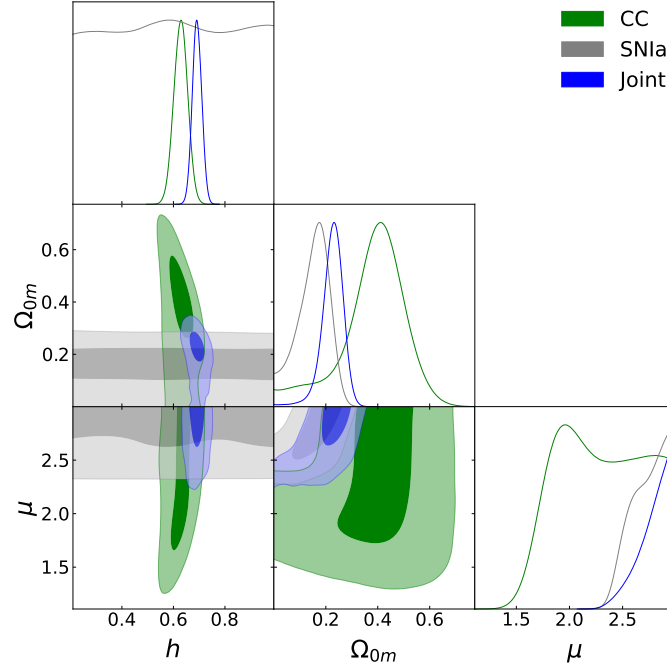


Figure 1. 2D likelihood contours at 68% and 99.7% CL, alongside the corresponding 1D posterior distribution of the free parameters, in fractional cosmology.

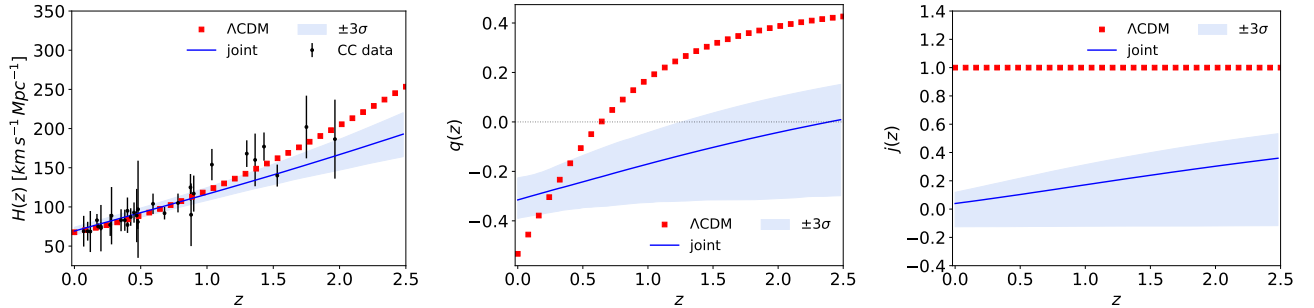


Figure 2. Left to right: reconstruction of the $H(z)$, $q(z)$, and $j(z)$, in fractional cosmology represent the results of Λ CDM cosmology with $h = 0.6766$ and $\Omega_{m0} = 0.3111$ (Aghanim & et. al. 2020).

subject to the restriction

$$G(x_1, x_2, A) := A^2 + (1 - \mu)A - \frac{1}{4}(x_1 + x_2)(2A + |1 - \mu|)^2 = 0. \quad (43)$$

As a plausible physical conditions we assume $0 \leq \Omega_m := \frac{x_1(2A + |1 - \mu|)^2}{4A^2} \leq 1$, $x_2 \geq 0$, $A \geq 0$. The physical parameter region we have considered is $1 \leq \mu \leq 3$.

Generically, evaluated at a fixed point P , we have

$$\rho_m(t) = \frac{3x_1(2A + |1 - \mu|)^2}{32\pi G t^2}, \rho_r(t) = \frac{3x_2(2A + |1 - \mu|)^2}{32\pi G t^2}, H(t) = \frac{A}{t}.$$

Therefore, we have two physical observables defined as the dimen-

sionless densities

$$\Omega_m = \frac{x_1(2A + |1 - \mu|)^2}{4A^2}, \quad \Omega_r = \frac{x_2(2A + |1 - \mu|)^2}{4A^2}, \quad (44)$$

and the deceleration parameter, which can be written as

$$q = -1 + \frac{1}{A} - \frac{(2A + |1 - \mu|)^2(3x_1(\mu - 3A + 1) + 2x_2(2\mu - 6A + 1))}{12A^2(-\mu + 2A + 1)}. \quad (45)$$

In Tab. 2 the equilibrium points of system (40), (41) and (42) which satisfy the restriction (43) are given.

In table 3 are presented the asymptotic values of the cosmological

Label	(x_1, x_2, A)	Existence	Eigenvalues	Stability	$\nabla G(x_1, x_2, A) _P$
P_1	$(0, 0, 0)$	$1 \leq \mu \leq 3$	$\{0, \mu + 1, \frac{2}{3}(2\mu + 1)\}$	Source	$(-\frac{ 1-\mu ^2}{4}, -\frac{ 1-\mu ^2}{4}, 1-\mu)$
P_2	$(0, -\frac{(2\mu+1)(4\mu-7)}{(2\mu+1+3 1-\mu)^2}, \frac{1}{6}(2\mu+1))$	$1 \leq \mu \leq \frac{7}{4}$	$\{0, \frac{1}{2}, -\frac{(2\mu+1)(4\mu-7)}{3(\mu-4)}\}$	Saddle	$(-\frac{1}{36}(2\mu+1+3 1-\mu)^2, -\frac{1}{36}(2\mu+1+3 1-\mu)^2, -\frac{2\mu^2+\mu+(\mu-4) 1-\mu +1}{2\mu+1+3 1-\mu })$
P_3	$(-\frac{8(\mu-2)(\mu+1)}{(2+2\mu+3 1-\mu)^2}, 0, \frac{\mu+1}{3})$	$1 \leq \mu < \frac{5}{2}$	$\{0, -\frac{2}{3}, -\frac{2(\mu-2)(\mu+1)}{\mu-5}\}$	Sink	$(-\frac{1}{36}(2\mu+2+3 1-\mu)^2, -\frac{1}{36}(2\mu+2+3 1-\mu)^2, \frac{2(\mu^2-1)-(\mu-5) 1-\mu }{2\mu+2+3 1-\mu })$
P_4	$(0, 0, \mu-1)$	$1 \leq \mu \leq 3$	$\{0, 2(2-\mu), \frac{2}{3}(7-4\mu)\}$	Source for $\mu < \frac{7}{4}$ Saddle for $\frac{7}{4} < \mu < 2$ Sink for $\mu > 2$	$(-\frac{1}{4}(2\mu-2+ 1-\mu)^2, -\frac{1}{4}(2\mu-2+ 1-\mu)^2, \mu-1)$

Table 2. Equilibrium points of system (40), (41) and (42). The physical parameter region is $1 \leq \mu \leq 3$. The existence condition is $0 \leq \frac{x_1(2A+|1-\mu|)^2}{4A^2} \leq 1, x_2 \geq 0, A \geq 0$.

Label	Ω_m	Ω_r	H	q	Solution	$a(t) = (t/t_U)^A$
P_1	Indeterminate	Indeterminate	0	Indeterminate	Static universe	$a(t) = \text{constant}$
P_2	0	$\frac{7-4\mu}{2\mu+1}$	$\frac{2\mu+1}{6t}$	$-\frac{2\mu-5}{2\mu+1}$	Power-law (decelerated if $\mu < \frac{5}{2}$) Power-law (accelerated if $\mu > \frac{5}{2}$)	$a(t) = (t/t_U)^{(2\mu+1)/6}$
P_3	$\frac{2(2-\mu)}{\mu+1}$	0	$\frac{\mu+1}{3t}$	$-\frac{\mu-2}{\mu+1}$	Power-law (decelerated if $\mu < 2$) Power-law (accelerated if $\mu > 2$)	$a(t) = (t/t_U)^{\frac{1+\mu}{3}}$
P_4	0	0	$\frac{\mu-1}{t}$	$-\frac{\mu-2}{\mu-1}$	Power-law (accelerated if $\mu < 1$ or $\mu > 2$) Power-law (decelerated if $1 < \mu < 2$)	$a(t) = (t/t_U)^{\mu-1}$

Table 3. Equilibrium points of system (40), (41) and (42). The physical parameter region is $1 \leq \mu \leq 3$.

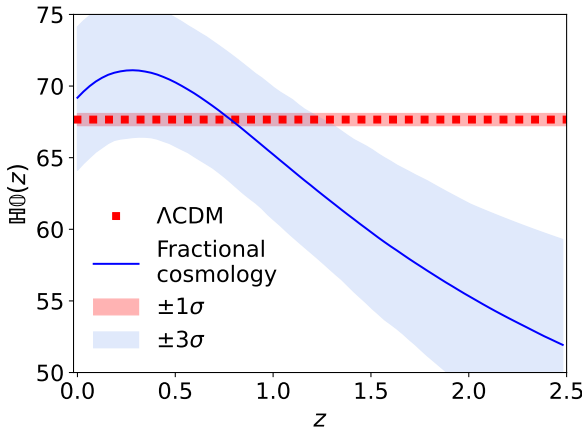


Figure 3. $H_0(z)$ diagnostic for fractional cosmology and its comparison against Λ CDM model.

parameter for the equilibrium points of system (40), (41) and (42), and the asymptotic expression of the scale factor.

For the best fit value $\mu = 2.839$, the late-time attractor, and the equilibrium points corresponding to the cosmological solutions summarized in table 4.

Following (Hewitt & Wainwright 1992; Nilsson & Uggla 1996; Goliath et al. 1998), we solve the restriction locally around the equilibrium points. This formulation will enable us to achieve a good understanding of the global structure of the reduced phase space.

One eigenvalue is always zero due to the restriction (43). The expression $G(x_1, x_2, A) = 0$ defines a singular surface, with

$$\nabla G(x_1, x_2, A) = \left(-\frac{1}{4}(2A + |1-\mu|)^2, -\frac{1}{4}(2A + |1-\mu|)^2, 2A + 1 - \mu - (x_1 + x_2)(2A + |1-\mu|) \right). \quad (46)$$

Notice that the gradient is different from zero at each point P_i if

$\mu \neq 1$. Therefore we can solve locally the restriction for each point P_1, P_2 and P_3 , say for $x_2 \geq 0$. Hence,

$$x_2 = \frac{4A(-\mu + A + 1)}{(2A + |1-\mu|)^2} - x_1. \quad (47)$$

Notice that replacing (47) in (45), we acquire

$$q = \frac{4\mu^2 - 5\mu + 6A^2 - 13\mu A + 13A + 1}{6A^2 - 3\mu A + 3A} - \frac{x_1(-\mu + 3A + 1)(2A + |1-\mu|)^2}{12A^2(-\mu + 2A + 1)}. \quad (48)$$

The dimensionless energy densities of matter and radiation reduces to

$$\Omega_m = \frac{x_1(2A + |\mu - 1|)^2}{4A^2}, \quad (49)$$

$$\Omega_r = 1 - \frac{(\mu - 1)^2 x_1}{4A^2} - \frac{\mu + x_1|\mu - 1| - 1}{A} - x_1. \quad (50)$$

Moreover, in the physical parameter region is $1 \leq \mu \leq 3$, we obtain the two-dimensional dynamical system

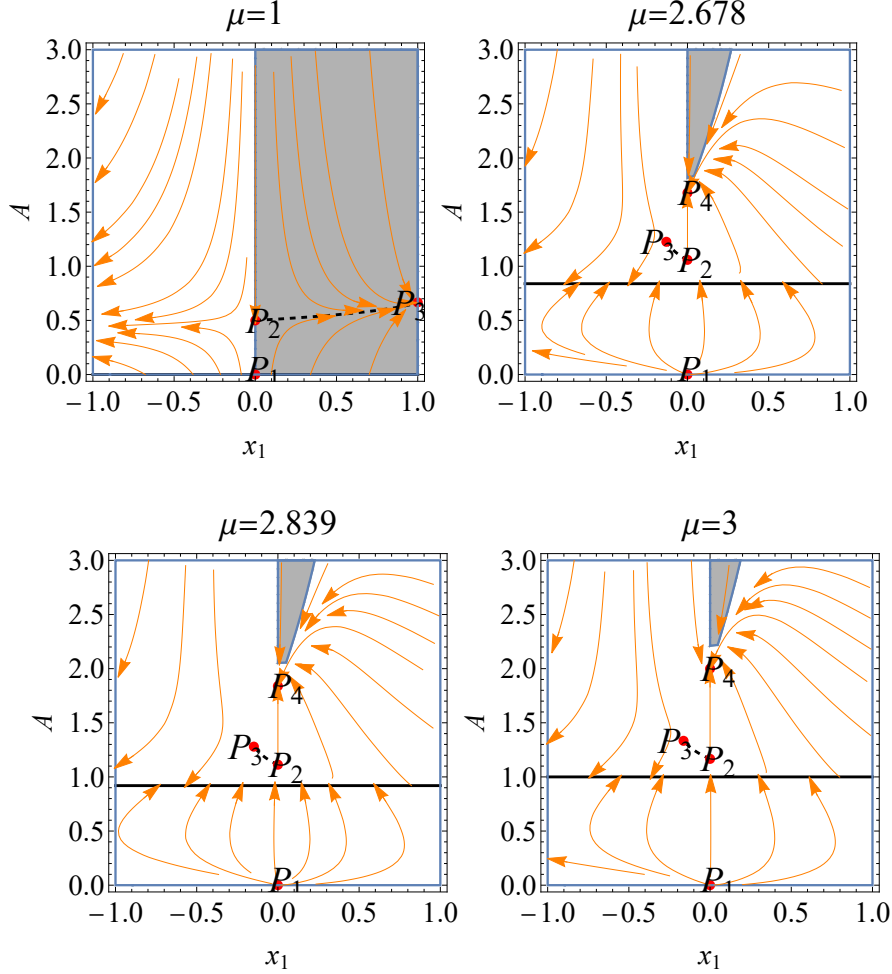
$$\frac{dx_1}{d\tau} = \frac{1}{3}x_1 \left[3\mu + \frac{6A(10A - 3)}{\mu + 2A - 1} + \frac{2A(2A(x_1 + 1) - 3)}{\mu - 2A - 1} - A(x_1 + 25) - \mu x_1 + x_1 + 3 \right], \quad (51)$$

$$\frac{dA}{d\tau} = \frac{1}{12(2A + 1 - \mu)} \left[12A^3(x_1 - 4) - 8A^2(-\mu(x_1 + 8) + x_1 + 5) - (\mu - 1)A(16\mu + (\mu - 1)x_1 + 8) - (\mu - 1)^3 x_1 \right], \quad (52)$$

defined on the phase plane

$$\left\{ (x_1, A) \in \mathbb{R}^2 : 0 \leq x_1 \leq 1, A \geq 0, 0 \leq \frac{4A(-\mu + A + 1)}{(\mu + 2A - 1)^2} - x_1 \leq 1 \right\}. \quad (53)$$

(x_1, x_2, A)	Eigenvalues	Solution
$(0, 0, 0)$	$\{0., 3.839, 4.452\}$	$\rho_m(t) \rightarrow 0, \rho_r(t) \rightarrow 0, H(t) \rightarrow 0$
$(0, -0.195601, 1.113)$	$\{0, \frac{1}{2}, 8.35181\}$	$\rho_m(t) \rightarrow 0, \rho_r(t) \rightarrow -\frac{0.0964524}{t}, H(t) \rightarrow \frac{1.113}{t}$ (nonphysical)
$(-0.147996, 0., 1.27967)$	$\{0, -\frac{2}{3}, 2.98095\}$	$\rho_m(t) \rightarrow -\frac{0.0854376}{t^2}, \rho_r(t) \rightarrow 0., H(t) \rightarrow \frac{1.27967}{t}$ (nonphysical)
$(0., 0., 1.839)$	$\{0., -1.678, -2.904\}$	$\rho_m(t) \rightarrow 0., \rho_r(t) \rightarrow 0., H(t) \rightarrow \frac{1.839}{t}$

Table 4. Cosmological solutions represented by equilibrium points for the best-fit value $\mu = 2.839$.**Figure 4.** Phase flow of the reduced system (51) and (52). The shadowed region corresponds to $0 \leq x_2 \leq 1$.

The equilibrium points of the reduced system are the same presented in Table 2, where we now omit the zero eigenvalues. The singular line $A = (1 - \mu)/2 \leq 0$ is not on the physical region (the physical parameter region is $1 \leq \mu \leq 3$).

Now that we locally solved the constraint to linear order, the eigenvalues and eigenvectors of the remaining locally unconstrained system are then listed.

(i) The eigensystem of $P_1 : (x_1, A) = (0, 0)$ (eigenvalues in first row; eigenvectors second row) is $\begin{pmatrix} \mu + 1 & \frac{2}{3}(2\mu + 1) \\ \{-\frac{4}{\mu-1}, 1\} & \{0, 1\} \end{pmatrix}$.

(ii) The eigensystem of $P_2 : (x_1, A) = (0, \frac{1}{6}(2\mu + 1))$ is $\begin{pmatrix} \frac{1}{2} & -\frac{(2\mu+1)(4\mu-7)}{3(\mu-4)} \\ \{-\frac{4(16\mu^2-17\mu-26)}{(5\mu-2)^2}, 1\} & \{0, 1\} \end{pmatrix}$.

(iii) The eigensystem of $P_3 : (x_1, A) = \left(-\frac{8(\mu-2)(\mu+1)}{(5\mu-1)^2}, \frac{\mu+1}{3}\right)$ is $\begin{pmatrix} -\frac{2}{3} & -\frac{2(\mu-2)(\mu+1)}{\mu-5} \\ \{-\frac{12(\mu-2)(\mu+1)(15\mu-11)}{(5\mu-1)^3}, 1\} & \{\frac{36(\mu-1)(\mu+7)}{(5\mu-1)^3}, 1\} \end{pmatrix}$.

(iv) The eigensystem of $P_4 : (x_1, A) = (0, \mu - 1)$ is $\begin{pmatrix} 4 - 2\mu & \frac{2}{3}(7 - 4\mu) \\ \{\frac{4}{9(\mu-1)}, 1\} & \{0, 1\} \end{pmatrix}$.

In Fig. 4 a phase flow of the reduced system (51) and (52) is presented. The physical part of the phase plane, $x_2 \geq 0$, is represented by a shaded region in the phase planes. It is confirmed that on the interval $1 \leq \mu \leq 3$, P_1 is a source, P_2 is a saddle (it is nonphysical for $\mu > \frac{7}{4}$) and P_3 is a sink (it is nonphysical for $\mu > \frac{5}{2}$). P_4 satisfies $a(t) = (t/t_U)^{\frac{1+\mu}{3}}$, which is physical for $1 \leq \mu < \frac{5}{2}$. Evaluating the dimensionless energy densities Ω_m , Ω_r of matter and radiation, and the Hubble parameter, we have $\Omega_m = -\frac{2(\mu-2)}{\mu+1}$, $\Omega_r = 0$, $H = \frac{\mu+1}{3t}$.

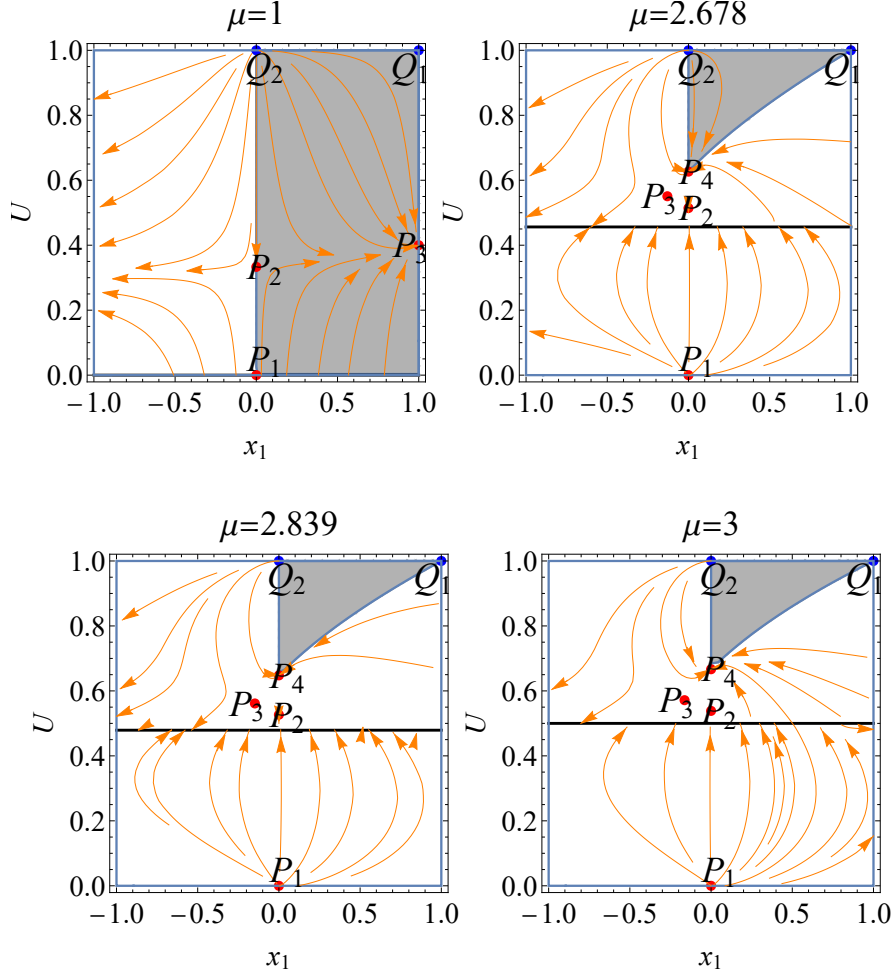


Figure 5. Phase flow of the reduced system (54) and (55). The shadowed region corresponds to $0 \leq x_2 \leq 1$.

and $q = -\frac{\mu-2}{\mu+1}$. It is a power-law (decelerated) late-time attractor for $\mu < 2$. Moreover, for $\mu > 1$ the more interesting solution is P_4 that, as is presented in Figure 4, it is the physical attractor for $\mu > 2$. Moreover, the point P_4 satisfies $a(t) = (t/t_U)^{\mu-1}$. It can be a source for $\mu < \frac{7}{4}$, or a saddle for $\frac{7}{4} < \mu < 2$ or a sink for $\mu > 2$. This point does not exist in G.R. (for which $\mu = 1$). The cosmological observable are $\Omega_m = 0$, $\Omega_r = 0$, $H = \frac{\mu-1}{t}$ and $q = -\frac{\mu-2}{\mu-1}$. This solution is accelerated power-law if $\mu < 1$ or $\mu > 2$, or decelerated power-law if $1 < \mu < 2$.

The previous system is not compact for A , so we define $U = A/(1+A)$ to obtain the dynamic system

$$\frac{dx_1}{d\tau} = \frac{1}{3}x_1 \left[(3-x_1)(\mu-1) + \frac{2U(U(2x_1+5)-3)}{U^2+\mu(U-1)^2-1} + \frac{6U(13U-3)}{(U-1)(-\mu+(\mu-3)U+1)} + \frac{U(x_1+25)}{U-1} \right], \quad (54)$$

$$\frac{dU}{d\tau} = \frac{1}{12} \left[\frac{8U^2(U(2x_1+5)-3)}{\mu(U-1)+U+1} + \mu^2(U-1)^2x_1 + x_1 - \mu(U-1)(U(5x_1+16)-2x_1) + U(2U(x_1-20)-5x_1+8) \right], \quad (55)$$

defined on

$$\left\{ (x_1, U) \in [0, 1]^2, 0 \leq \frac{4U(\mu(U-1)+1)}{(1-\mu+(\mu-3)U)^2} - x_1 \leq 1 \right\}. \quad (56)$$

In Fig. 5 a phase flow of the reduced system (54) and (55) is presented. Additionally to P_1, P_2, P_3 and P_4 , there appear two points at infinity. The point $Q_1 : (x_1, U) = (1, 1)$ that is a saddle and the point $Q_2 : (x_1, U) = (0, 1)$ that is a local source.

For the analysis of the unstable manifold of P_2 , we consider the quantities u, v defined in Appendix C, E.Q.s. (C1), and defines the graph $(u, g(u))$ in (C2) which satisfies the differential equation (C3). The cosmological solution associated to the unstable manifold of P_2 determines a curve in the physical space $(t^2\rho_m, t^2\rho_r, tH)$ given by

$$t^2\rho_m(t) = -\frac{(\mu(16\mu-17)-26)u(5\mu+6g(u)+6u-2)^2}{24\pi(2-5\mu)^2G}, \quad (57)$$

$$t^2\rho_r(t) = \frac{3\left((2-5\mu)^2+4(\mu(16\mu-17)-26)u\right)\left(\frac{\mu}{3}+g(u)+u+\frac{1}{6}\right)^2}{8\pi(2-5\mu)^2G} + \frac{3(1-\mu)\left((2-5\mu)^2+4((17-16\mu)\mu+26)u\right)\left(\frac{\mu}{3}+g(u)+u+\frac{1}{6}\right)}{8\pi(2-5\mu)^2G} + \frac{3(\mu(16\mu-17)-26)(\mu-1)^2u}{8\pi(2-5\mu)^2G}, \quad (58)$$

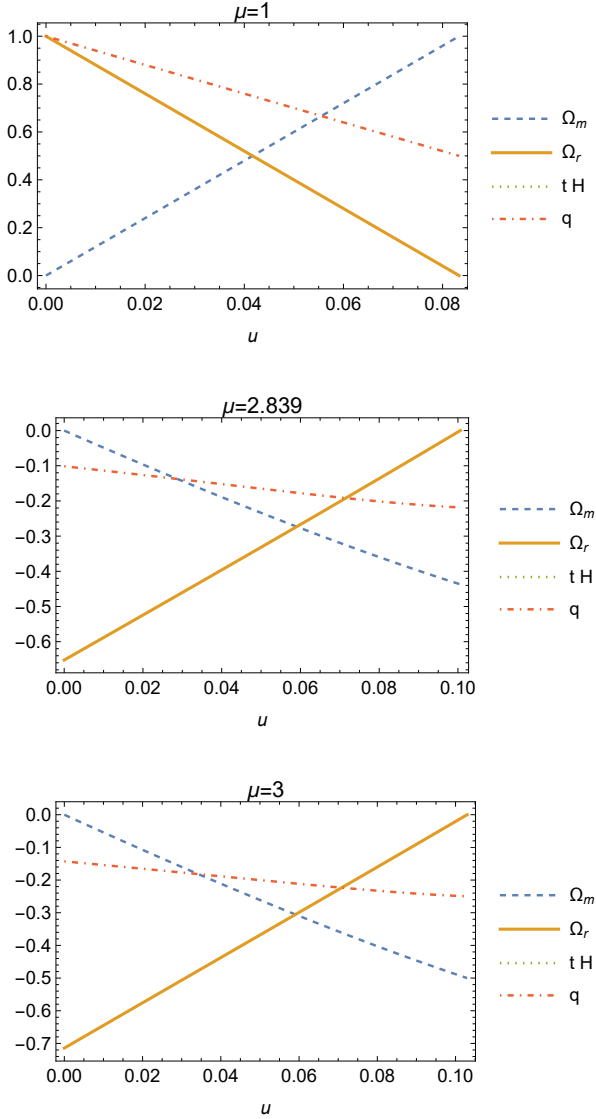


Figure 6. Evolution of Ω_m , Ω_r , tH and q vs u for different values of μ , as the flow moves along the unstable manifold connecting the saddle point P_2 with the sink P_3 . For $\mu > 7/4$ point P_2 becomes nonphysical leading to negative Ω_r , as well as P_3 which for $\mu > 5/2$ leads to negative Ω_m . P_3 becomes unstable for $\mu > 2$ emerging the late-time accelerated power-law solution P_4 for $\mu > 2$. The middle and lower panels show that we have acceleration without Dark Energy.

$$tH(t) = \frac{\mu}{3} + g(u) + u + \frac{1}{6}. \quad (59)$$

such that

$$\Omega_m = -\frac{4(\mu(16\mu - 17) - 26)u(5\mu + 6g(u) + 6u - 2)^2}{(2 - 5\mu)^2(2\mu + 6g(u) + 6u + 1)^2}, \quad (60)$$

$$\Omega_r = \frac{4(\mu(16\mu - 17) - 26)u(5\mu + 6g(u) + 6u - 2)^2}{(2 - 5\mu)^2(2\mu + 6g(u) + 6u + 1)^2} + \frac{6 - 6\mu}{2\mu + 6g(u) + 6u + 1} + 1. \quad (61)$$

In figure 6 is presented the evolution of Ω_m , Ω_r , tH and q vs u for the values $\mu \in \{1.0, 2.839, 3.0\}$. Observe that as $\mu \approx 1$, at P_3 , $\Omega_r \sim 0$, $\Omega_m \sim 1$, in complete analogy with the CDM model ($\Lambda = 0$). For $\mu > 7/4$ point P_2 becomes nonphysical leading to negative Ω_r ,

as well as P_3 which for $\mu > 5/2$ leads to negative Ω_m . P_3 becomes unstable for $\mu > 2$ emerging the late-time accelerated power-law solution P_4 for $\mu > 2$.

7 BIANCHI I UNIVERSE

In the Misner variables, the L.R.S. Bianchi I spacetime is described by the line element

$$ds^2 = -N^2(t) dt^2 + e^{2\alpha(t)} \left(e^{2\beta(t)} dx^2 + e^{-\beta(t)} (dy^2 + dz^2) \right), \quad (62)$$

where α is the scale factor for the three-dimensional hypersurface and β is the anisotropic parameter while N is the lapse function. For $\beta \rightarrow 0$, the line element (62) reduces to the spatially flat FLRW geometry. The Lagrangian of GR, i.e. the Ricci scalar, is calculated as

$$R = \frac{1}{N^2} \left(6\ddot{\alpha} - 6\dot{\alpha}\frac{\dot{N}}{N} + 12\dot{\alpha}^2 + \frac{3}{2}\dot{\beta}^2 \right). \quad (63)$$

The fractional effective action can be written in the form

$$S_{\text{eff}} = \frac{1}{\Gamma(\alpha)} \int_0^t \left[\frac{3}{8\pi G N^2(\tau)} \left(\ddot{\alpha}(\tau) - \frac{\dot{\alpha}(\tau)\dot{N}(\tau)}{N(\tau)} + 2\dot{\alpha}^2(\tau) + \frac{1}{4}\dot{\beta}^2(\tau) \right) + e^{3\alpha(\tau)} \mathcal{L}_m \right] (t - \tau)^{\mu-1} N(\tau) d\tau. \quad (64)$$

Varying the action (64) for $q_i \in \{N, \alpha, \beta\}$, and using the gauge $N = 1$ after the variation, we obtain from the Euler-Poisson equations, the equations of motion

$$\dot{\alpha}^2 + \frac{(1-\mu)\dot{\alpha}}{t} - \frac{1}{4}\dot{\beta}^2 = \frac{8\pi G}{3}\rho, \quad (65)$$

$$\ddot{\alpha} + \frac{(1-\mu)\dot{\alpha}}{t} + \frac{3}{2}\dot{\alpha}^2 + \frac{3}{8}\dot{\beta}^2 + \frac{(\mu-2)(\mu-1)}{2t^2} = -4\pi G p, \quad (66)$$

$$\dot{\beta} \left(3\dot{\alpha} + \frac{1-\mu}{t} \right) + \ddot{\beta} = 0, \quad (67)$$

where $\rho = \sum_i \rho_i$ and $p = \sum_i p_i$ denotes the total energy density and total pressures of the matter fields. Now $H = \dot{\alpha}$ and $\sigma = \dot{\beta}/2$ are respectively the Hubble parameter and the anisotropy parameter.

Therefore, the field equations can alternatively be written as

$$H^2 + \frac{(1-\mu)H}{t} - \sigma^2 = \frac{8\pi G}{3} \sum_i \rho_i, \quad (68)$$

$$\dot{H} + \frac{(1-\mu)H}{t} + \frac{3}{2}H^2 + \frac{(\mu-2)(\mu-1)}{2t^2} + 3\sigma^2 = -4\pi G \sum_i p_i, \quad (69)$$

$$\dot{\sigma} + 3\sigma \left(H + \frac{1-\mu}{3t} \right) = 0, \quad (70)$$

and we consider separated conserved equations

$$\dot{\rho}_i + 3 \left(H + \frac{1-\mu}{3t} \right) (\rho_i + p_i) = 0. \quad (71)$$

As before, it is expected that the continuity equation for a perfect fluid is the energy conservation law for the matter, which is followed using the Bianchi identity. For $\alpha \neq 1$, (71) also yields modified continuity equations, only if

$$\frac{8\pi G}{3} \sum_i p_i = \frac{2(\mu-3)H}{t} + H^2 - \frac{(\mu-2)(\mu-1)}{t^2} - \sigma^2. \quad (72)$$

Eliminating $\sum_i p_i$ and $\sum_i \rho_i$ from (68), (69) and (72), results in the cancellation of the σ -terms. Therefore, obtaining the master equation

(23) that has the solution (24) where c_1 is an integration constant depending of μ , the value of H today, H_0 and the age of the Universe, t_U . That also leads to $a(t) \simeq t^{\frac{1}{6}(-2\mu+\sqrt{8\mu(2\mu-9)+105+9})}$ for large t . For $\mu \notin \{1, 2\}$ and for large t , we acquire $q < 0$, and then we have late-time acceleration without DE.

7.1 Dynamical Systems and Stability Analysis

Using the equation of state $p_i = w_i \rho_i$, where $w_i \neq -1$ are constants, and defining dimensionless variables

$$\Omega_i = \frac{8\pi G \rho_i}{3H^2}, \quad \Sigma = \frac{\sigma}{H}, \quad A = tH, \quad (73)$$

which satisfies

$$1 - \frac{(\mu-1)}{A} = \Sigma^2 + \sum_i \Omega_i, \quad (74)$$

and taking the new derivative $f' = \dot{f}/H$, we obtain for $\mu \neq 1$,

$$\Omega'_j = \Omega_j \left[(2q - 3w_j - 1) + (w_j + 1) \left(1 - \Sigma^2 - \sum_i \Omega_i \right) \right], \quad (75)$$

$$\Sigma' = \Sigma \left[(q - 2) + \left(1 - \Sigma^2 - \sum_i \Omega_i \right) \right], \quad (76)$$

$$A' = 1 - A(1 + q), \quad (77)$$

where the deceleration parameter is found from Eq. (23) (valid for FLRW and Bianchi I metrics) as

$$q := -1 - \frac{\dot{H}}{H^2} = 2 + \frac{2(\mu-4)}{A} - \frac{(\mu-2)(\mu-1)}{A^2}. \quad (78)$$

Assuming $\mu \neq 1$ and using (74) to eliminate the A , we have

$$q = 2 - \frac{(\mu-2)}{(\mu-1)} \left(1 - \Sigma^2 - \sum_i \Omega_i \right) + \frac{2(\mu-4)}{(\mu-1)} \left(1 - \Sigma^2 - \sum_i \Omega_i \right), \quad (79)$$

To compare with the standard model we impose that the universe components are two ($n = 2$), CDM ($\rho_1 = \rho_m, w_1 = w_m = 0$) and radiation ($\rho_2 = \rho_r, w_2 = w_r = 1/3$), which in our modified scenario, the dimensionless energy densities evolve according to

$$\Omega'_m = \Omega_m \left[4 - \Omega_m - \Omega_r - \Sigma^2 - \frac{2(\mu-2) \left(\Omega_m + \Omega_r + \Sigma^2 - 1 \right)^2}{\mu-1} - \frac{4(\mu-4) \left(\Omega_m + \Omega_r + \Sigma^2 - 1 \right)}{\mu-1} \right], \quad (80)$$

$$\Omega'_r = \Omega_r \left[2 - \frac{4}{3} \left(\Omega_m + \Omega_r + \Sigma^2 - 1 \right) - \frac{2(\mu-2) \left(\Omega_m + \Omega_r + \Sigma^2 - 1 \right)^2}{\mu-1} - \frac{4(\mu-4) \left(\Omega_m + \Omega_r + \Sigma^2 - 1 \right)}{\mu-1} \right], \quad (81)$$

$$\Sigma' = \frac{\Sigma \left(1 - \Omega_m - \Omega_r - \Sigma^2 \right)}{\mu-1} \left[(\mu-2) \left(\Sigma^2 + \Omega_m + \Omega_r \right) + 2\mu - 7 \right]. \quad (82)$$

The equilibrium points of the system (80), (81) and (82) are presented in Table 5.

In figure 7 is presented a phase space of the system (80), (81) and (82) for $\mu \in \{2.678, 2.839, 3\}$. The possible late-time attractors are the equilibrium point B with $\Omega_m = 0$, $\Omega_r = 0$, $\Sigma = 0$, $A = \mu - 1$ and $q = \frac{3\mu-8}{\mu-1}$ which is a sink for $1 < \mu < 8/3$; the equilibrium point E with $\Omega_m = -\frac{\mu+\sqrt{\mu(49\mu-242)+337-9}}{4(\mu-2)}$,

$\Omega_r = 0$, $\Sigma = 0$, $A = \left(-5\mu + \sqrt{\mu(49\mu-242)+337} + 17 \right) / 6$, $q = -\frac{\sqrt{49\mu^2-242\mu+337+\mu-9}}{8(\mu-2)}$. It is a sink for $\mu > 8/3$; and the equilibrium point F with $\Omega_m = \frac{-\mu+\sqrt{\mu(49\mu-242)+337+9}}{4(\mu-2)}$, $\Omega_r = 0$, $\Sigma = 0$, $A = \left(-5\mu - \sqrt{\mu(49\mu-242)+337} + 17 \right) / 6$ and $q = \frac{\sqrt{49\mu^2-242\mu+337-\mu+9}}{8(\mu-2)}$, which is a sink for $\mu > 2$.

To close the ideas presented in this paper, we finally show alternative calculations (see Subsec. 3.2 and Appendix B) in order to make more efficient the numerical computation, in particular with the free parameter constraints. In this case we invert (26) and substitute into (B1) and (B2), in order to obtain an alternative form for $H(z)$ and $q(z)$ where now is used a new notation for the free parameters h , μ^* and t_U^* . In this formulation, we have, for the different priors, the best-fit parameters summarized in Fig. 8. This new approach works for FLRW and Bianchi I models and deserves further investigation.

8 SUMMARY AND DISCUSSIONS

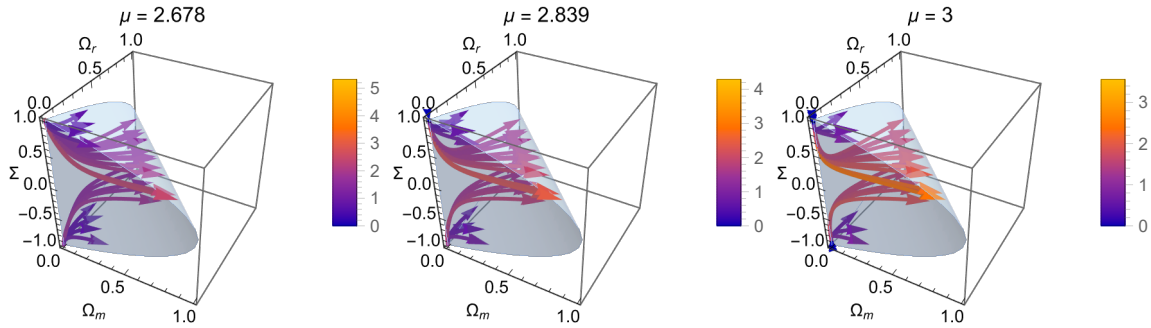
We study the recent proposition of fractional cosmology to elucidate if the theory is capable of reproducing the observed dynamics of the Universe, in specific, if it is capable of predicting the Universe's acceleration and giving some clues about the fundamental nature of the dark energy. We implement constraints through cosmic chronometers, Type Ia Supernovae, and joint analysis and summarized our results in Fig. 1 and Table 1. The fractional parameter prefers $\mu = 2.839^{+0.117}_{-0.193}$ for a joint analysis which suggests a solid presence of fractional calculus in the dynamical equations of cosmology; however, it generates crucial differences as it is possible to observe from Figs 2. Of course, we expect this behaviour to have an accelerated Universe at late times. From one side, the term $(1-\mu)H/t$ acts like an extra source of mass, closing the Universe and not allowing the observed dynamics, in particular, the Universe acceleration at late times if $\mu < 2$, but, for $\mu > 2$, we can have an accelerated power-law solution. Furthermore, from Figs. 2 it is possible to notice that the fractional constant f can act like the object that causes the Universe acceleration. It is possible to observe from $H(z)$ and $q(z)$ essential differences when we compare them with the standard model, mainly at high redshifts. In addition, the jerk parameter also shows that the causative of the Universe acceleration is not a cosmological constant because, at $z = 0$, the fractional parameter does not converge to $j = 1$; this coincides with recent studies that suggest that it is not a Λ the cause of the Universe acceleration (Zhao et al. 2017). Moreover, the Universe's age obtained under this scenario is $t_U = 33.617^{+3.411}_{-4.511}$ Gyrs based on our Joint analysis, around 2.4 times larger than the age of the Universe expected under the standard paradigm. However, this value does not contradict the minimum bound expected for the universe age imposed by globular clusters, and, as far as we know, the maximum bound does not exist and is model-dependent. Finally, we observe a trend of H_0 to the value obtained by SH0ES (Riess et al. 2019) at current times, and in agreement with Planck's value (Aghanim & et. al. 2020) for $z \lesssim 1.5$. However, a discrepancy between both values in the region $1.5 < z < 2.5$ holds, such that H_0 tension is not fully resolved.

Additionally, we have presented a dynamical system and stability analysis to explore the phase-space under the assumption of different μ parameters. This formulation enabled us to achieve a good understanding of the global structure of the reduced phase space. One late-time attractor have $a(t) = (t/t_U)^{\frac{1+\mu}{3}}$, which is physical for $1 \leq \mu < \frac{5}{2}$. Evaluating the dimensionless energy densities Ω_m , Ω_r

Label	Ω_m	Ω_r	Σ	A	q	Stability
A	0	0	-1	Infinity	2	Source for $1 < \mu < 3$
B	0	0	0	$\mu - 1$	$\frac{3\mu-8}{\mu-1}$	Sink for $1 < \mu < \frac{8}{3}$ Source for $\mu > \frac{7}{2}$ Saddle for $\frac{8}{3} < \mu < \frac{23}{8}$ or $\frac{23}{8} < \mu < \frac{7}{2}$
C	0	$-\frac{\mu+\sqrt{\mu(25\mu-131)+187}-7}{3(\mu-2)}$	0	$\frac{1}{3}(-4\mu + \sqrt{\mu(25\mu-131)+187} + 13)$	$-\frac{2\sqrt{25\mu^2-131\mu+187}+\mu+8}{9(\mu-2)}$	Saddle
D	0	$-\frac{\mu+\sqrt{\mu(25\mu-131)+187}+7}{3(\mu-2)}$	0	$\frac{1}{3}(-4\mu - \sqrt{\mu(25\mu-131)+187} + 13)$	$\frac{2\sqrt{25\mu^2-131\mu+187}+\mu+8}{9(\mu-2)}$	Saddle
E	$-\frac{\mu+\sqrt{\mu(49\mu-242)+337}-9}{4(\mu-2)}$	0	0	$\frac{1}{6}(-5\mu + \sqrt{\mu(49\mu-242)+337} + 17)$	$-\frac{\sqrt{49\mu^2-242\mu+337}+\mu-9}{8(\mu-2)}$	Sink for $\mu > \frac{8}{3}$ Saddle for $1 < \mu < 2$ or $2 < \mu < \frac{8}{3}$
F	$-\frac{\mu+\sqrt{\mu(49\mu-242)+337}+9}{4(\mu-2)}$	0	0	$\frac{1}{6}(-5\mu - \sqrt{\mu(49\mu-242)+337} + 17)$	$\frac{\sqrt{49\mu^2-242\mu+337}-\mu+9}{8(\mu-2)}$	Sink for $\mu > 2$ Source for $1 < \mu < 2$
G	0	0	1	Infinity	2	Source for $1 < \mu < 3$
H	0	0	$-\frac{\sqrt{7-2\mu}}{\sqrt{\mu-2}}$	$\frac{(\mu-2)(\mu-1)}{3(\mu-3)}$	$-\frac{\mu-5}{\mu-2}$	Saddle
I	0	0	$\frac{\sqrt{7-2\mu}}{\sqrt{\mu-2}}$	$\frac{(\mu-2)(\mu-1)}{3(\mu-3)}$	$-\frac{\mu-5}{\mu-2}$	Saddle

Table 5. Equilibrium points of the system (80), (81) and (82). We assume $1 \leq \mu \leq 3$. The eigenvalues are summarized in table 6.

Label	λ_1	λ_2	λ_3
A	$\frac{12}{\mu-1} - 6$	2	3
B	$2 - \frac{5}{\mu-1}$	$6 - \frac{10}{\mu-1}$	$\frac{16}{3} - \frac{10}{\mu-1}$
C	$\frac{\sqrt{25\mu^2-131\mu+187}-5\mu+5}{18-9\mu}$	$-\frac{4(\mu(25\mu+\sqrt{\mu(25\mu-131)+187}-131)-7\sqrt{\mu(25\mu-131)+187})}{9(\mu-2)(\mu-1)}$	$-\frac{5\mu+\sqrt{\mu(25\mu-131)+187}+5}{9(\mu-2)}$
D	$\frac{9}{-5\mu+\sqrt{\mu(25\mu-131)+187}+5}$	$\frac{4(\mu(-25\mu+\sqrt{\mu(25\mu-131)+187}+131)-7\sqrt{\mu(25\mu-131)+187})}{9(\mu-2)(\mu-1)}$	$\frac{5\mu+\sqrt{\mu(25\mu-131)+187}-5}{9(\mu-2)}$
E	$\frac{-7\mu+\sqrt{\mu(49\mu-242)+337}+7}{8(\mu-2)}$	$-\frac{7\mu+\sqrt{\mu(49\mu-242)+337}+7}{12(\mu-2)}$	$-\frac{\mu(49\mu+\sqrt{\mu(49\mu-242)+337}-242)-9\sqrt{\mu(49\mu-242)+337}+337}{4(\mu-2)(\mu-1)}$
F	$\frac{\mu(-49\mu+\sqrt{\mu(49\mu-242)+337}+242)-9\sqrt{\mu(49\mu-242)+337}-337}{4(\mu-2)(\mu-1)}$	$-\frac{7\mu+\sqrt{\mu(49\mu-242)+337}-7}{8(\mu-2)}$	$-\frac{7\mu+\sqrt{\mu(49\mu-242)+337}-7}{12(\mu-2)}$
G	$\frac{12}{\mu-1} - 6$	2	3
H	$\frac{2}{\mu-2}$	$\frac{3}{\mu-2}$	$\frac{60}{\mu-1} - \frac{18}{\mu-2} - 12$
I	$\frac{2}{\mu-2}$	$\frac{3}{\mu-2}$	$\frac{60}{\mu-1} - \frac{18}{\mu-2} - 12$

Table 6. Eigenvalues of the Jacobian matrix evaluated at the equilibrium points of the system (80), (81) and (82).**Figure 7.** Phase space of the system (80), (81) and (82) for some values of μ . The gray surface correspond to the boundary $1 = \Sigma^2 + \sum_i \Omega_i$ corresponding to $A \rightarrow \infty$.

of matter and radiation, and the Hubble parameter, we identify P_3 with a power-law (decelerated) late-time attractor for $\mu < 2$. Moreover, for $\mu > 1$ exists an additional point not present in GR with $a(t) = (t/t_U)^{\mu-1}$ which can be a source for $\mu < \frac{7}{4}$ or a saddle for $\frac{7}{4} < \mu < 2$, or a sink for $\mu > 2$. Evaluating the dimensionless densities Ω_m , Ω_r of matter and radiation, and the Hubble parameter, we identify P_4 with an accelerated power-law if $\mu < 1$ or $\mu > 2$, or decelerated power-law if $1 < \mu < 2$.

For the Bianchi I metric, the possible late-time attractors are all isotropic ($\Sigma = 0$). They are the equilibrium point B which is a sink

for $1 < \mu < 8/3$; the equilibrium point E , which is a sink for $\mu > 8/3$; and the equilibrium point F , which is a sink for $\mu > 2$.

Moreover, the new approach of fractional calculus opens new windows to affront calculations that traditional calculus can not resolve. For example, the problem of determining the energy density value for the cosmological constant can be attached to this approach or even applied to the standard model field to make its calculations efficient. As we demonstrate in this research, fractional calculus contributes with a constant that acts as the causative of the Universe's acceleration without the need to add no natural term into the field

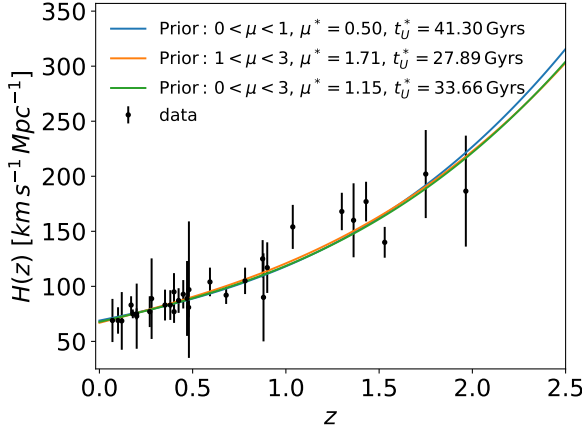


Figure 8. $H(z)$ reconstruction using Eqs. (25), (26) and (B1) and best-fit values (μ^* , t_U^*) for different priors on μ .

equations. Indeed, if we had written the Einstein Field equations in the fractional setup, the Friedmann equations naturally contained a constant term, predicting the existence of a late time Universe in acceleration contrary to the standard approach. Moreover, as it is possible to observe, the model presents differences in comparison with the standard model at high redshifts being the smoking gun to differentiate among the theories.

Finally, from a mathematical perspective, it is expected that many physical phenomena and systems are better described by fractional differential equations rather than the equivalent integer-order equations. Since the set of integers is a set of measure zero, and the real numbers are a set of measure one, nature prefers non-integer dimensions and parameters. Therefore, we recommend that the community study other approaches like this presented in the paper to understand the Universe's acceleration with another mathematical background. For example, in fractional calculus, the mathematical richness generates the Λ -like term originated in the corrections due to the fractional index μ of the fractional derivative, which could resolve the energy density problem. In future studies, it is possible to aboard the fractional Einstein equation using linear perturbations theory to understand acoustic peaks of the CMB, the power spectrum and inflation. However, this will be presented elsewhere.

ACKNOWLEDGMENTS

We thank the anonymous referee for thoughtful remarks and suggestions. M.A.G.-A. acknowledges support from cátedra Marcos Moshinsky and Universidad Iberoamericana for support with the S.N.I. grant; G.F.A. acknowledges support from DINVP and Universidad Iberoamericana. A.H.A. thanks to the support from Luis Aguilar, Alejandro de León, Carlos Flores, and Jair García of the Laboratorio Nacional de Visualización Científica Avanzada. G.L. was funded by Vicerrectoría de Investigación y Desarrollo Tecnológico (Vridt) at U.C.N. and through Concurso De Pasantías De Investigación Año 2022, Resolución Vridt N 040/2022 under the Project “The Hubble constant tension: some ways to alleviate it” and through Resolución Vridt No. 054/2022. G.L. acknowledges the invitation of organizers of the conference “Tensions in Cosmology”, held on Sep 7 - Sep 12, 2022 - in Corfu, Greece, where part of these results was presented. J.M. acknowledges the support from ANID REDES 190147.

DATA AVAILABILITY

The data underlying this article were cited in Section 4.

REFERENCES

- Aghanim N., et. al. 2020, *A&A*, 641, A6
 Barrientos E., Mendoza S., Padilla P., 2021, *Symmetry*, 13, 174
 Calcagni G., 2010a, *JHEP*, 03, 120
 Calcagni G., 2010b, *Phys. Rev. Lett.*, 104, 251301
 Calcagni G., 2013, *JCAP*, 12, 041
 Calcagni G., 2017a, *JHEP*, 03, 138
 Calcagni G., 2017b, *Phys. Rev. D*, 96, 046001
 Calcagni G., 2021a, *Mod. Phys. Lett. A*, 36, 2140006
 Calcagni G., 2021b, *Class. Quant. Grav.*, 38, 165005
 Calcagni G., 2021c, *Classical and Quantum Gravity*, 38, 165006
 Calcagni G., De Felice A., 2020, *Phys. Rev. D*, 102, 103529
 Calcagni G., Kuroyanagi S., 2021, *JCAP*, 03, 019
 Calcagni G., Kuroyanagi S., Tsujikawa S., 2016, *JCAP*, 08, 039
 Calcagni G., Kuroyanagi S., Marsat S., Sakellariadou M., Tamanini N., Tasi-nato G., 2019, *JCAP*, 10, 012
 Carroll S. M., 2001, *Living Rev. Rel.*, 4, 1
 Debnath U., Jamil M., Chattopadhyay S., 2012, *International Journal of Theoretical Physics*, 51, 812
 Debnath U., Chattopadhyay S., Jamil M., 2013, *Journal of Theoretical and Applied Physics*, 7, 25
 Di Valentino E., et al., 2021a, *Class. Quant. Grav.*, 38, 153001
 Di Valentino E., et al., 2021b, *Astropart. Phys.*, 131, 102607
 Efstathiou G., 2021, *Mon. Not. Roy. Astron. Soc.*, 505, 3866
 El-Nabulsi R. A., 2005, *Electron. J. Theor. Phys.*, 2, 1
 El-Nabulsi R. A., 2007a, *Rom. J. Phys.*, 52, 163
 El-Nabulsi R. A., 2007b, *Rom. Rep. Phys.*, 59, 763
 El-Nabulsi R. A., 2008, *Electron. J. Theor. Phys.*, 5, 0103
 El-Nabulsi R. A., 2012, *Int. J. Theor. Phys.*, 51, 3978
 El-Nabulsi A. R., 2013a, *Indian J. Phys.*, 87, 835
 El-Nabulsi R. A., 2013b, *Can. J. Phys.*, 91, 618
 El-Nabulsi R. A., 2016a, *Int. J. Theor. Phys.*, 55, 625
 El-Nabulsi R. A., 2016b, *Rev. Mex. Fis.*, 62, 240
 El-Nabulsi R. A., 2017a, *Int. J. Theor. Phys.*, 56, 1159
 El-Nabulsi R. A., 2017b, *Commun. Theor. Phys.*, 68, 309
 El-Nabulsi R. A., 2017c, *Can. J. Phys.*, 95, 605
 Foreman-Mackey D., Hogg D. W., Lang D., Goodman J., 2013, *Publications of the Astronomical Society of the Pacific*, 125, 306
 Giusti A., 2020, *Phys. Rev. D*, 101, 124029
 Goliath M., Nilsson U. S., Uggla C., 1998, *Class. Quant. Grav.*, 15, 2841
 Hewitt C. G., Wainwright J., 1992, *Phys. Rev. D*, 46, 4242
 Jalalzadeh S., da Silva F. R., Moniz P. V., 2021, *Eur. Phys. J. C*, 81, 632
 Jalalzadeh S., Costa E. W. O., Moniz P. V., 2022, *Phys. Rev. D*, 105, L121901
 Jamil M., Momeni D., Rashid M. A., 2012, *J. Phys. Conf. Ser.*, 354, 012008
 Kilbas A., Srivastava H., Trujillo J., 2006, *North Holland Mathematical Studies*, 204
 Krishnan C., Ó Colgáin E., Sheikh-Jabbari M., Yang T., 2021, *Phys. Rev. D*, 103
 Lim S. C., 2006, *Physica A*, 363, 269
 Lim S. C., Eab C. H., 2019, *Fractional quantum fields*. De Gruyter, pp 237–256, doi:10.1515/9783110571721-010
 Moniz P. V., Jalalzadeh S., 2020, *Mathematics*, 8, 313
 Moresco M., et al., 2016, *JCAP*, 1605, 014
 Motta V., García-Aspeitia M. A., Hernández-Almada A., Magaña J., Verdugo T., 2021, *Universe*, 7, 163
 Nilsson U., Uggla C., 1996, *Class. Quant. Grav.*, 13, 1601
 Podlubny I., 1998, *Fractional Differential Equations*, Volume 198. Elsevier
 Rami E.-N. A., 2015, *Eur. Phys. J. Plus*, 130, 102
 Rasouli S. M. M., Jalalzadeh S., Moniz P. V., 2021, *Mod. Phys. Lett. A*, 36, 2140005
 Riess A. G., Filippenko A. V., Challis P., Clocchiatti A., Diercks A., et al., 1998, *The Astronomical Journal*, 116, 1009

Riess A. G., Casertano S., Yuan W., Macri L. M., Scolnic D., 2019, *Astrophys. J.*, 876, 85
 Roberts M. D., 2014, *SOP Trans. Theor. Phys.*, 1, 310
 Scolnic D. M., et al., 2018, *Astrophys. J.*, 859, 101
 Shchigolev V. K., 2011, *Commun. Theor. Phys.*, 56, 389
 Shchigolev V. K., 2013a, *Discontinuity, Nonlinearity, and Complexity*, 2, 115
 Shchigolev V. K., 2013b, *Mod. Phys. Lett. A*, 28, 1350056
 Shchigolev V. K., 2016, *Eur. Phys. J. Plus*, 131, 256
 Shchigolev V. K., 2021, *Mod. Phys. Lett. A*, 36, 2130014
 Tarasov V. E., 2013, *International Journal of Modern Physics B*, 27
 Torres I., Fabris J. C., Piattella O. F., Batista A. B., 2020, *Universe*, 6, 50
 Uchaikin V. V., 2013, *Fractional derivatives for physicists and Engineers*.

Higher Education Press
 V. Moniz P., Jalalzadeh S., 2020, *Challenging Routes in Quantum Cosmology*.
 World Scientific Publishing, Singapore, doi:10.1142/8540
 Vacaru S. I., 2010, *Int. J. Theor. Phys.*, 49, 2753
 Vacaru S. I., 2012a, *Chaos Solitons Fractals*, 45, 1266
 Vacaru S. I., 2012b, *Int. J. Theor. Phys.*, 51, 1338
 Valcin D., Jimenez R., Verde L., Bernal J. L., Wandelt B. D., 2021, *Journal of Cosmology and Astroparticle Physics*, 2021, 017
 Weinberg S., 1989, *Reviews of Modern Physics*, 61
 Zeldovich Y. B., 1968, *Soviet Physics Uspekhi*, 11
 Zhao G.-B., et al., 2017, *Nature Astron.*, 1, 627

APPENDIX A: DECELERATION PARAMETER AS A CLOSED FORMULA OF REDSHIFT.

Here we compute the deceleration parameter, using Eq. (20), which yields to

$$q(z) = -1 + \frac{(z+1)}{E(z)} \left\{ \frac{2f^2 F(z)^2}{(\mu-1)(z+1)E(z)} + \frac{(E(z) + fF(z)) \left(-\frac{12f^3 F(z)^{\frac{4\mu}{3} + \frac{11}{3}}}{(\mu-1)(z+1)E(z)} + \frac{6f\Omega_{0m}(z+1)^2 F(z)^{\frac{\mu+8}{3}}}{E(z)} + \frac{8f\Omega_{0r}(z+1)^3 F(z)^3}{E(z)} + 9\Omega_{0m}(z+1)^2 F(z)^{\frac{\mu+5}{3}} + 12\Omega_{0r}(z+1)^3 F(z)^2 \right)}{6 \left(f^2 F(z)^{\frac{4(\mu+2)}{3}} + \Omega_{0m}(z+1)^3 F(z)^{\frac{\mu+5}{3}} + \Omega_{0r}(z+1)^4 F(z)^2 \right)} \right\}, \quad (A1)$$

where $E(z)$ function is given by (18).

APPENDIX B: ALTERNATIVE E AND DECELERATION PARAMETER

Alternative expressions for E and the deceleration parameter that makes use of the exact solution of (23) given by (24) are

$$E(t) = \frac{1}{H_0} \left[\frac{9-2\mu}{6t} + \frac{\sqrt{8\mu(2\mu-9)+105} \left(1 - \frac{2c_1}{t^{\sqrt{8\mu(2\mu-9)+105}+c_1}} \right)}{6t} \right], \quad (B1)$$

and

$$q(t) = -1 + \frac{-6c_1^2 \left(2\mu + \sqrt{8\mu(2\mu-9)+105} - 9 \right) + 6 \left(-2\mu + \sqrt{8\mu(2\mu-9)+105} + 9 \right) t^2 \sqrt{8\mu(2\mu-9)+105} - 24c_1 (\mu(8\mu-35) + 48) t^{\sqrt{8\mu(2\mu-9)+105}}}{\left(\left(-2\mu + \sqrt{8\mu(2\mu-9)+105} + 9 \right) t^{\sqrt{8\mu(2\mu-9)+105}} - c_1 \left(2\mu + \sqrt{8\mu(2\mu-9)+105} - 9 \right) \right)^2}. \quad (B2)$$

where c_1 is defined by (27), and the relation between t and z is obtained by inverting (26).

APPENDIX C: UNSTABLE MANIFOLD OF P_2

To find the unstable manifold of P_2 , we define

$$u = -\frac{(2-5\mu)^2 x_1}{64\mu^2 - 68\mu - 104}, \quad v = -\frac{\mu}{3} + A + \frac{21(5\mu+34)x_1}{64(\mu(16\mu-17)-26)} + \frac{25x_1}{64} - \frac{1}{6}. \quad (C1)$$

The graph

$$\{(u, v) : v = g(u), g(0) = g'(0) = 0\} \quad (C2)$$

locally gives the unstable manifold of P_2 , where g satisfies the differential equation

$$\begin{aligned}
& 4((17 - 16\mu)\mu + 26)(2 - 5\mu)^2 u(-\mu + 6g(u) + 6u + 4)(5\mu + 6g(u) + 6u - 2) \\
& \times \left[3(\mu + 1) - \left(\frac{4((17 - 16\mu)\mu + 26)u}{(2 - 5\mu)^2} + 25 \right) \left(\frac{\mu}{3} + g(u) + u + \frac{1}{6} \right) + \frac{2(2\mu + 6g(u) + 6u + 1)(5\mu + 15g(u) + 15u - 2)}{5\mu + 6g(u) + 6u - 2} \right. \\
& + \frac{6\left(\frac{\mu}{3} + g(u) + u + \frac{1}{6}\right) \left(2\left(\frac{4((17 - 16\mu)\mu + 26)u}{(2 - 5\mu)^2} + 1\right) \left(\frac{\mu}{3} + g(u) + u + \frac{1}{6} \right) - 3 \right)}{\mu - 6g(u) - 6u - 4} - \frac{4((17 - 16\mu)\mu + 26)\mu u}{(2 - 5\mu)^2} + \frac{4((17 - 16\mu)\mu + 26)u}{(2 - 5\mu)^2} \left. \right] g'(u) \\
& + (64\mu^2 - 68\mu - 104) \left\{ -36u^4(5\mu(2\mu(56\mu - 45) - 201) + 60(\mu(16\mu - 17) - 26)g(u) + 166) \right. \\
& - 6u^3((5\mu - 2)(\mu(\mu(400\mu - 459) - 138) - 532) + 6g(u)(\mu(4\mu(340\mu - 207) - 2649) + 72(\mu(16\mu - 17) - 26)g(u) + 470)) \\
& + u^2 \left[12g(u)(3g(u)(\mu(52(3 - 20\mu)\mu + 2403) + 36((17 - 16\mu)\mu + 26)g(u) - 466) - (5\mu - 2)(\mu(\mu(320\mu - 393) + 132) - 464)) \right. \\
& - (2 - 5\mu)^2(\mu(4\mu(20\mu - 9) - 69) - 218) \left. \right] \\
& + ug(u) \left[18g(u) \left(-((5\mu - 2)(\mu(\mu(80\mu - 79) + 182) - 156)) - 6g(u) \left(\mu(4\mu(20\mu + 31) - 293) + (32\mu^2 - 34\mu - 52)g(u) + 62 \right) \right) \right. \\
& - (2 - 5\mu)^2(\mu(80(\mu - 3)\mu + 357) - 116) \left. \right] \\
& + (2 - 5\mu)^2 g(u)(4\mu - 6g(u) - 7)(2\mu + 6g(u) + 1)(5\mu + 6g(u) - 2) - 648(\mu(16\mu - 17) - 26)u^5 \left. \right\} = 0. \tag{C3}
\end{aligned}$$

This paper has been typeset from a \LaTeX file prepared by the author.